Microscopically-Viewed Structural Change of Polyethylene during Isothermal Crystallization from the Melt I.
Time-Resolved FT-IR Spectral Measurements

Kohji Tashiro,[†] Sono Sasaki, Naomi Gose, and Masamichi Kobayashi

*Department of Macromolecular Science, Graduate School of Science, Osaka University,
Toyonaka, Osaka 560-0043, Japan*

ABSTRACT: Microscopically-viewed structural change of polyethylene (PE) in isothermal crystallization from the melt was investigated by the time-resolved measurements of high-resolution FT-IR spectra. The samples were a high-density PE and a linear low-density PE with *ca.* 17 ethyl branchings/1000 carbons. The latter was used to reduce the crystallization rate and to make structural change clearer than the case of the former sample. At the early stage of the isothermal crystallization, IR bands characteristic of the conformationally-disordered *trans* sequences were found to increase in intensity. After keeping the maximum for a while, the intensity of these disordered *trans* bands began to decrease and that of the regular *trans* bands characteristic of the orthorhombic crystal gradually increased instead. The FT-IR data showed that the conformationally-disordered short *trans* sequences appear at first in the random coils of the melt and these disordered *trans* sequences grow to the longer and regular *trans* sequences of the orthorhombic-type crystal. The disordered *trans* form is considered to play an important role as a kind of nucleus for the crystallization of the orthorhombic form.
    KEY WORDS   Polyethylene / Isothermal Crystallization / Time-Resolved Fourier Transform Infrared Measurement / Conformationally-Disordered *trans* Form /

In the study of polymer crystallization, clarification of the mechanism of nucleation and growth of lamellae has been one of the most important subjects. Investigations of crystallization mechanism viewed from the crystalline lamellar scale have been reported for many polymer materials.[1-11] The structural change during the isothermal crystallization of polyethylene (PE) has been also investigated extensively from the view points of lamellae and spherulite.[12-22] By carrying out the time-resolved measurements of the small-angle X-ray scattering (SAXS) during the isothermal crystallization of PE from the melt, Schultz *et al.* reported that single lamellae are generated at first in the melt and new crystallites grow between the existing single lamellae.[12,13] Based on the correlation function analysis of the SAXS data, Strobl *et al.* indicated that the crystallization starts with the generation of isolated lamellae and a continuous growth of the lamellar thickness occurs logarithmically with an elapse of time.[14-16] Their observation was different from the stepwise thickening of the lamellae reported by Barham and Keller.[17] Stein *et al.* investigated the isothermal crystallization behavior of the blend between high-density PE (HDPE) and low-density PE (LDPE) by time-resolved synchrotron-sourced SAXS measurements[18,19] and the small-angle light scattering.[20] The results were interpreted in such a way that the crystallization of the HDPE component first occurs and the spherulites fill the whole space of the sample and then the LDPE component crystallizes lately in the amorphous zone between the HDPE lamellar stacks with keeping the spherulite structure unchanged. These studies revealed the mechanism of the primary nucleation and the secondary crystal growth at the lamellar level. But the problem as to how the molecular chain conformation changes during crystallization has not yet been solved,

which seems quite important for the clarification of the essential features of the crystallization mechanism of PE.

In a series of papers[23-31] we have studied the crystallization behavior of the PE homopolymer and the blends between deuterated high-density PE (DHDPE) and hydrogenous PE with various degrees of ethyl side-chain branchings. On slow cooling from the melt, these blends show either the phase segregation or the cocrystallization depending on the degree of ethyl side-chain branchings of the H species. To understand the crystallization behavior of the blends, the crystallization mechanism of the PE homopolymer itself needs to be clarified at first. In previous papers,[28,29] we carried out the time-resolved measurements of the SAXS and FT-IR during the isothermal crystallization of PE and these different types of data were compared. The infrared crystalline bands could be observed with some time delay before the appearance of the invariant Q evaluated from the SAXS data. We could thus imagine the concrete change of the molecular and crystalline structures during the crystallization from the melt. But at that time the resolution power of the vibrational frequency was not very high and the time interval of the spectral measurement was also not short enough to trace the structural change in detail. In addition to these problems, we have to improve the temperature jump apparatus for more perfect reproducibility of the temperature changes. The solution of these problems will make it clearer how the molecular chain conformation changes in isothermal crystallization.

In the discussion of such a structural change the concrete assignment of the infrared (and Raman) bands is needed as useful information on the *trans* and *gauche* conformational sequences. Recently we succeeded in obtaining the detailed structural information on the orthorhombic-to-hexagonal transition occurring in the narrow temperature region just below the melting point

---

of PE sample by carrying out the time-resolved X-ray diffraction and the FT-IR and FT-Raman spectral measurements.[32] In particular, IR bands characteristic of the hexagonal phase or the conformationally-disordered (CONDIS) phase were revealed experimentally for the first time. This allowed us to speculate that the conformationally disordered *trans* chain segments might appear during the transition from the melt to the regular orthorhombic phase. Therefore, we carried out time-resolved FT-IR measurements with high resolution power to clarify the structural changes during the isothermal crystallization process of PE samples, as will be reported in the present paper.

EXPERIMENTAL

Samples

We used a HDPE and a linear low-density PE (LLDPE), supplied by Exxon Chemicals Co., Ltd. The characterization of these samples was made as follows.

	M_w	M_n	M_w/M_n	Ethyl branching/1000C
HDPE	126 K	24 K	5.3	1
LLDPE	75 K	37 K	2.0	17

PE crystallizes very rapidly depending on the degree of supercooling. To perform the experiment of temperature jump more easily and stably, the crystallization rate should be slower. This is possible by choosing small ΔT, where ΔT is a degree of supercooling defined as $\Delta T = T_m^0 - T_c$. The T_c is the predetermined crystallization temperature and the T_m^0 is the equilibrium melting temperature. But temperature control is actually very difficult for such small ΔT as 0.5—1.0°C with small temperature fluctuation (0.1—0.2°C) in the temperature jump experiment. Therefore, we employed another idea: by introducing some short branching, the crystallization rate may be reduced to some extent. Of course, the essential features of the crystallization behavior should not be different from the normal HDPE case. In the present study, therefore, we utilized not only HDPE but also LLDPE with low degree of ethyl branching. It should be noticed that the LLDPE sample could be used for the present study, because it has enough sharp distribution of the molecular weight and the side branching. The well-developed lamellar and spherulite structures are obtained for this sample crystallized from the melt, which are very similar to those observed for HDPE, as already reported in the previous papers.[23–31]

The samples were melted and pressed on a hot plate at *ca.* 160°C and then cooled slowly to room temperature.

Temperature Jump Method

In the isothermal crystallization experiments, it is quite important to cool the samples as fast as possible from the molten state to T_c. The temperature reached after this jump should be constant and stable.[15,16] Therefore, temperature-jump apparatus was designed carefully for the time-resolved FT-IR measurement. The details of the apparatus are described in the previous papers.[28] At that time the cooling rate was about 600°C min^{-1} but, by making the sample holder part smaller, the cooling rate

of 4200°C min^{-1} could be attained in the present study. In this experiment monitoring the sample temperature was very important. Therefore, we embedded the thermocouple "into" the sample and recorded the temperature change directly by an x–y recorder. After the jump was completed the temperature was stable with sufficiently small fluctuation (ca. ±0.2°C at maximum). The equilibrium melting temperature T_m^0 of PE is reported to be about 145°C.[33] But this should be dependent on the degree of branching and the T_m^0 has not yet been known exactly for the samples used in the experiment. Therefore the temperature T_c^0, at which the crystallization bands begin to be observed in the infrared spectral measurement during the slow cooling from the melt, was used tentatively instead of the T_m^0. That is to say, ΔT was re-defined as $\Delta T = T_c^0 - T_c$. Therefore, it should be emphasized here that "ΔT" used in the present study is not the conventionally-defined "degree of supercooling" but a kind of practical measure of the degree of supercooling for the crystallization phenomenon. The T_c^0 for HDPE and LLDPE were 123 and 109°C, respectively, as estimated from the temperature-dependent measurement of the infrared spectra in the crystallization process from the melt.[23,24]

FT-IR Spectral Measurements

FT-IR spectra were measured by a Bio-Rad FTS-60A/896 Fourier-transform infrared spectrometer equipped with an MCT detector in the rapid scan mode at a rate of 0.3—1.0 s/spectrum with the spectral resolution of 2 cm^{-1}.

Separation of the Overlapped Infrared Bands

To evaluate the integrated intensity of each component in the overlapped infrared bands, curve separation was performed thoroughly.[32] The band component was assumed to be a weighted mixture of the Lorentzian and Gaussian functions and the variables (the relative weight of these two functions, the height, the width, and the peak position) were adjusted by a nonlinear least-squares method so that the totally summed spectral profile was fitted to the observed pattern as well as possible. The program installed in the Bio-Rad FTS-60A/896 FT-IR spectrometer was used.

In the previous paper,[32] we found the components of bands necessary for the curve separation of characteristic states such as the melt, orthorhombic phase, or hexagonal phase. This was applied to the separation of the complicated spectra measured in the present study. The signal-to-noise (S/N) ratio of the spectra was estimated to be about 5% for all the frequency regions, although the S/N depends on the conditions of spectral measurements such as the setting of the sample, the sample thickness (relative absorbance), the environmental atmosphere (humidity), etc. The influence of bands of water vapor was also taken into consideration by referring to the spectra of pure water vapor measured independently.

RESULTS AND DISCUSSION

Infrared Spectral Change During Crystallization

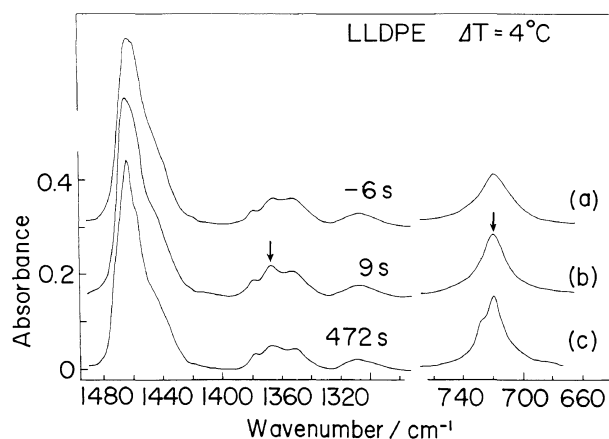Figure 1 shows the IR spectra picked up from a series

486

Figure 1. FT-IR spectra of LLDPE sample, extracted from a series of spectra measured at constant time interval during the isothermal crystallization from the melt at $\Delta T = 4°C$ and cooling rate of *ca.* 600°C min^{-1}. The time indicated in this figure was measured from the starting point ($t = 0$), defined as the time when the temperature reached just the predetermined crystallization point (T_c). (a), (b), and (c) correspond to the spectra of the melt, the intermediate state (disordered *trans* form) and the orthorhombic crystal, respectively, although an overlapping of the spectra between the different states must be considered more or less. The bands pointed by arrows in (b) correspond to the disordered *trans* form discussed in the text.
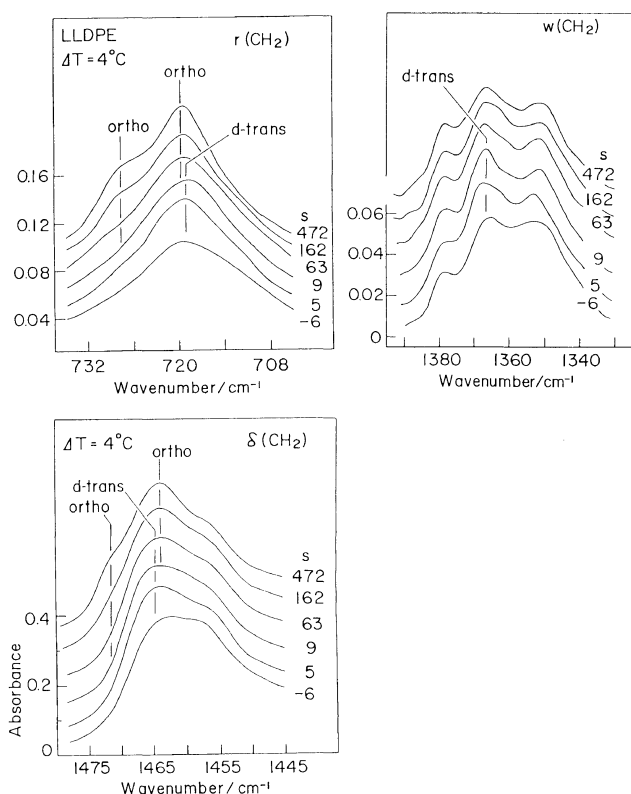

Figure 2. Time dependence of the IR spectra enlarged in the frequency regions of the CH$_2$ rocking (r), wagging (w), and bending (δ) modes of LLDPE measured during the isothermal crystallization from the melt at $\Delta T = 4°C$ and cooling rate of *ca.* 600°C min^{-1}.

of spectra taken by the time-resolved measurement during the isothermal crystallization from the melt of LLDPE sample at $\Delta T = 4°C$, where the time indicated in this figure was measured from the starting point ($t = 0$), defined as the time when the temperature reached just the predetermined crystallization point (T_c). The three spectra in this figure are assumed respectively to be
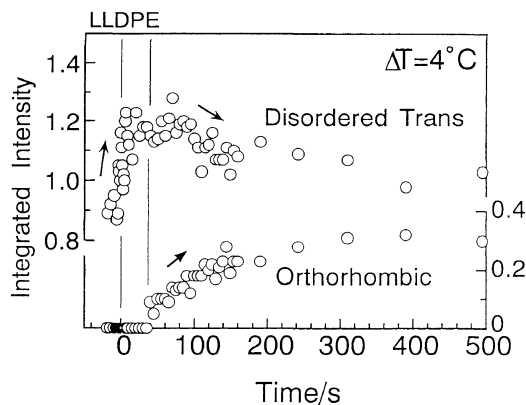

Figure 3. Time dependence of the integrated intensity of IR bands measured for LLDPE during the isothermal crystallization from the melt at $\Delta T = 4°C$ and cooling rate of *ca.* 600°C min^{-1}. The vibrational frequency of the analyzed disordered *trans* band is 1368 cm^{-1} and that of the orthorhombic phase is 728 cm^{-1}.

characteristic of (a) the melt (including some effect from the intermediate state already), (b) the intermediate state (described later), and (c) the orthorhombic crystal (at high temperature or with low degree of crystallinity). Figure 2 shows the time dependence of the IR spectra in the frequency regions of the CH$_2$ rocking, wagging, and bending modes measured for LLDPE sample at $\Delta T = 4°C$. As seen in Figure 1, the spectra of the intermediate state are different from those of the melt and the orthorhombic crystal. This can be observed more clearly in Figure 2. Immediately after the temperature jump, some bands, pointed out by arrows in Figure 1, begin to increase in intensity and then decrease again in the crystallization. In the previous study,[32] we found the IR bands characteristic of the hexagonal phase or the CONDIS phase of PE as follows:

> short and disordered *trans* segments 1466, 719 cm^{-1}
> kink ($\cdots$TTGTGTT$\cdots$) contained
>   in the disordered *trans* segments 1368, 1306 cm^{-1}
> local double-*gauche* defect 1352 cm^{-1}
>   ($\cdots$TTGGTT$\cdots$)

The bands pointed by arrows in the figure correspond to these characteristic bands. That is to say, at the beginning of the isothermal crystallization, the bands characteristic of the melt decrease in intensity and the bands corresponding to the above-listed disordered *trans* form increase in intensity, and after that the exchange of intensity begins to occur between the bands of disordered *trans* form and the bands intrinsic to the long and regular *trans* segments (the orthorhombic crystalline bands) at 1471 and 728 cm^{-1}.

To make quantitative analysis, the overlapped bands were separated into the components as described in the experimental section. The integrated intensities of the separated band components are plotted against the temperature in Figure 3. The starting point ($t = 0$) was defined as the time when the temperature reached just the predetermined crystallization point (T_c). The intensity of the disordered *trans* band at 1368 cm^{-1} began to increase during the temperature jump and kept increasing even after the temperature reached the T_c. After keeping at maximum for a while, this band intensity began to decrease gradually. In this time region, the long and

regular *trans* band at 728 cm^{-1} appeared and increased in intensity. Such a tendency could be seen similarly for $\Delta T = 5$, 6, 7, and 9°C. For example, the case with $\Delta T = 6$°C is shown in Figure 4.

In Figures 1—4, the temperature changed at a rate of *ca.* 600°C min^{-1}. Because the crystallization rate is very high in the PE case, the thermal equilibrium might not be perfectly attained but change even partly during the temperature jump. To confirm the appearance of the disordered *trans* band more definitely, we measured the IR spectra again at higher cooling rate of 4200°C min^{-1}. Although the observed spectra are not reproduced here, the spectral changes were essentially the same with those in Figures 1 and 2; that is intensity change could be reconfirmed for the bands intrinsic to the melt, the disordered *trans* form and the regular orthorhombic form. Intensity changes evaluated from the spectra are plotted in Figure 5, where three different ΔT's were employed. It should be noticed here that, in order to enhance the temperature jump rate more drastically, the
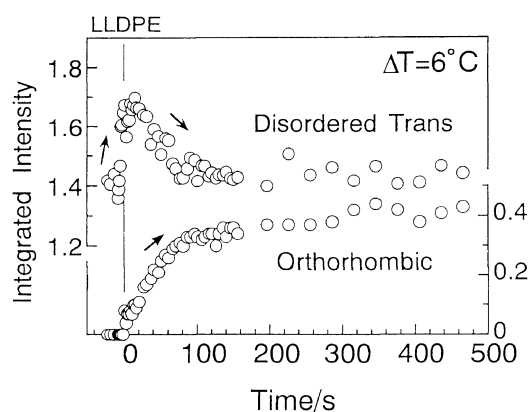

Figure 4. Time dependence of the integrated intensity of IR bands measured for LLDPE during the isothermal crystallization from the melt at $\Delta T = 6$°C and cooling rate of *ca.* 600°C min^{-1}. The vibrational frequency of the analyzed disordered *trans* band is 1368 cm^{-1} and that of the orthorhombic phase is 728 cm^{-1}.

sample thickness and the hole size of the sample holder (necessary for the IR beam transmission) were decreased by about a half from those used in the above-mentioned 600°C min^{-1} case, making the measurement very severe. This severe condition (in particular the reduction of sample size or the decrease of the transmission energy) reduced the S/N ratio of the obtained spectra and besides the effect of the water vapor became more significant because of the difficulty of getting good balance of the optical conditions between the reference and the sample. Therefore the data plotted in Figure 5 are scattered to some extent compared with those in Figures 3 and 4. The optical path of the incident infrared beam deviated slightly before and after the jump of the sample holder due to the very small size of the sample. The data obtained before the jump ($t < 0$ s) thus could not be used in this case of 4200°C min^{-1}.

Although the measurement conditions are appreciably different from the two cases, the results obtained at 4200°C min^{-1} for $\Delta T = 4$°C may be said to be essentially the same as Figure 3 (600°C min^{-1}). As ΔT becomes smaller, the peak position of the curve showing the intensity change of the disordered *trans* band shifted to the longer time direction, reflecting the lower crystallization rate at the smaller degree of supercooling. For the $\Delta T = 2$°C, the disordered *trans* band began to increase in intensity "after" the sample temperature reached almost the stable value. In other words, we can say definitely that the disordered *trans* bands appear first in the "isothermal" crystallization process prior to the appearance of the orthorhombic-type *trans* bands.

People might consider that the appearance of the disordered *trans* bands is observed only for the LLDPE sample used here. Figure 6 shows a similar plot of the infrared band intensities measured for the HDPE sample. In this case, the crystallization rate was quite high and so the time-resolved measurement was very difficult. But, as seen in Figure 6, the appearance of the disordered *trans* bands at 1368 cm^{-1} and the intensity exchange
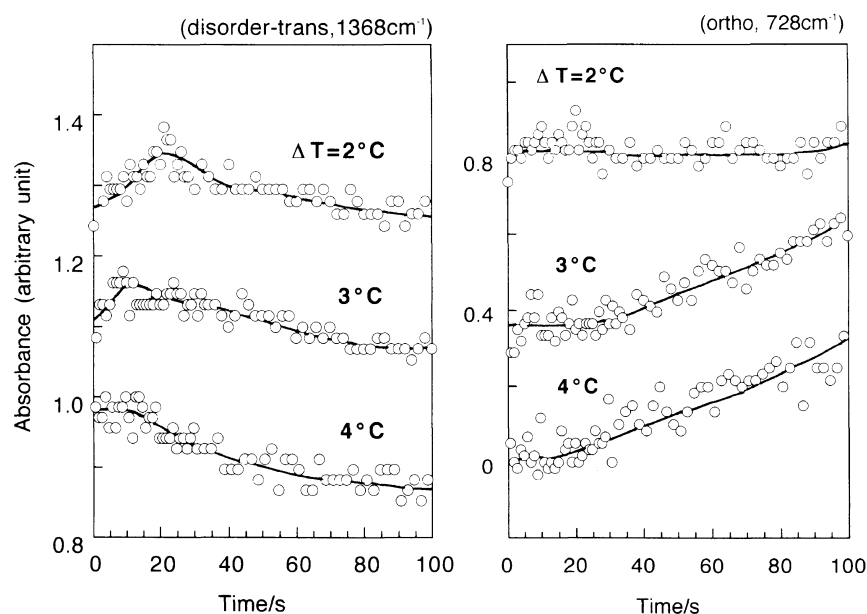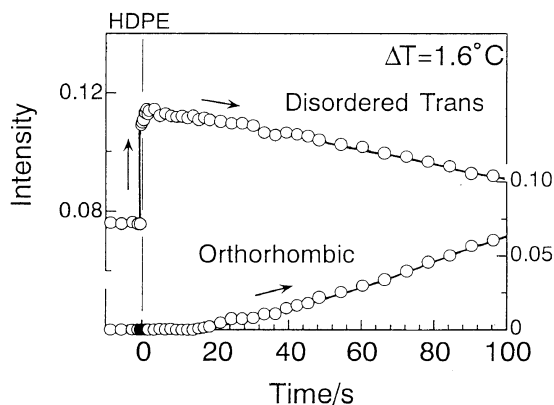

Figure 5. Time dependence of the intensity of IR bands at 1368 and 728 cm^{-1} measured for LLDPE during the isothermal crystallization from the melt at $\Delta T = 2$, 3, and 4°C and cooling rate of 4200°C min^{-1}. Because the optical path of the incident infrared beam deviated slightly before and after the jump of the sample holder due to the too small size of the sample, the data obtained before the jump ($t < 0$ s) could not be used in this case.

Figure 6. Time dependence of the intensity of IR bands measured for HDPE during the isothermal crystallization from the melt at $\Delta T = 1.6°C$ and cooling rate of ca. $3800°C\,min^{-1}$. The vibrational frequency of the analyzed disordered *trans* band is $1368\,cm^{-1}$ and that of the orthorhombic phase is $728\,cm^{-1}$.
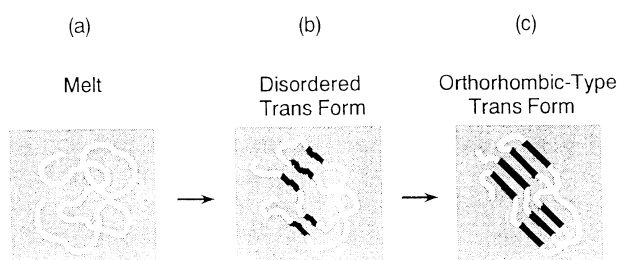

Figure 7. An illustrated structural change of the random coil to orthorhombic-type lamella occurring in the crystallization process of PE.

between the disordered *trans* band and the regular *trans* band can be observed clearly by the small ΔT and the higher temperature jump rate ($3800°C\,min^{-1}$).

From all the data shown in Figures 1—6, we may conclude that in isothermal crystallization from the melt the chain conformational change occurs from the random coil to the regular planar-zigzag form *via* the disordered *trans* form. In parallel to this infrared spectral measurement, we carried out also the time-resolved small-angle X-ray scattering (SAXS) measurements during isothermal crystallization of the various PE samples at almost the same temperature jump rate of $600°C\,min^{-1}$. Although the quantitative analysis of the SAXS data is now being made, the time dependence of the invariant Q, which is defined as the integrated value of Lp-corrected scattering intensity over the whole wave vector range, and the observation of the peak corresponding to the long spacing between the stacked lamellae indicated that the formation and growth of crystalline lamellae start in the time region of the structural transformation from the disordered *trans* to regular orthorhombic form. By taking into account the data of the present FT-IR and SAXS experiments, the structural change in the early stage of isothermal crystallization may be illustrated in Figure 7. The details will be published as soon as possible.

trans-gauche Population in the Melt

In order to understand why the disordered *trans* segments appear before the crystallization into the orthorhombic form, we need to clarify the behavior of the disordered *trans* bands in the molten state. FT-IR
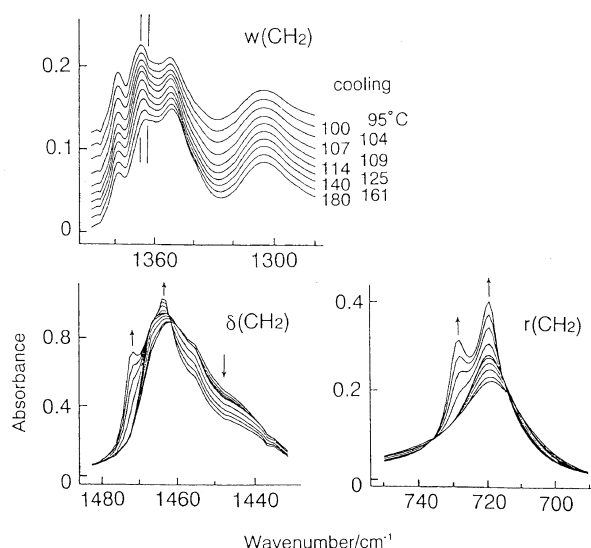

Figure 8. IR spectral change in the frequency regions of the CH_2 bending (δ), wagging (w), and rocking (r) modes measured for LLDPE during the slow cooling from the melt.
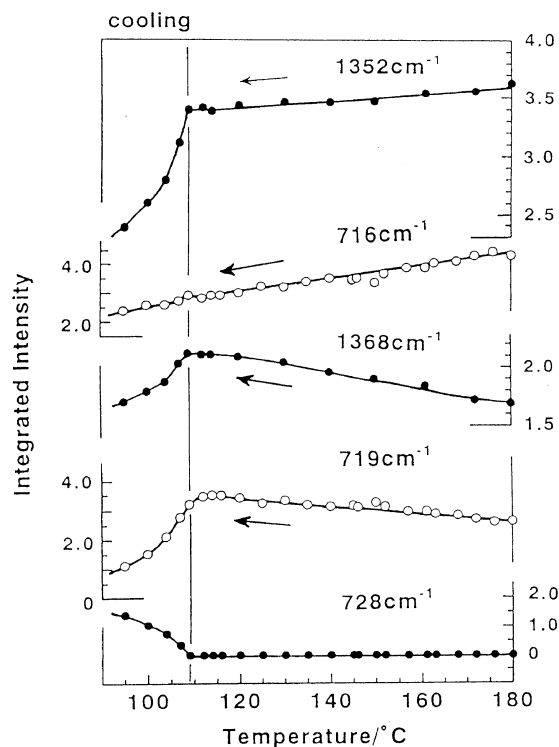

Figure 9. Temperature dependence of the integrated intensity of the IR bands of LLDPE during the slow cooling from the melt.

spectral measurement was performed during the slow-cooling from the melt to the room temperature. It should be notified here that the measurement was made in a static mode with the step-wise decrease of the temperature, different from the above mentioned time-resolved measurement. As seen in Figure 8, the IR spectra in the CH_2 bending [$\delta(CH_2)$], wagging [$w(CH_2)$], and rocking [$r(CH_2)$] mode regions change continuously even in the molten state. In Figure 9 is shown the temperature dependence of the integrated intensities of the bands indicated above. In the temperature region above the crystallization temperature, the 1352 cm^{-1} band of the local double *gauche* form and the 716

489

cm^{-1} band of the single *gauche* form are observed to decrease the intensity gradually as the temperature decreases. The bands related with the short *trans*-zigzag segments (including kink structure) at 1368 and 719 cm^{-1} increased instead. These bands reflecting the conformationally disordered chain segments decrease in intensity rapidly below the crystallization temperature, and the regular *trans*-zigzag bands of the orthorhombic crystal phase at 728 (and 720) cm^{-1} increase in intensity. An intensity exchange between the bands characteristic of the *gauche*-rich (1352, 716 cm^{-1}) and *trans*-rich (1368, 719 cm^{-1}) segments is considered to reflect the change of the conformational distribution from the *gauche* to the *trans* isomers. The distribution is governed approximately by the Boltzmann's law $[\exp(-\Delta E/kT)]$ where ΔE is energy difference between the *trans* and *gauche* forms. That is to say, as the temperature is lowered "in" the molten state, the population of short and disordered *trans* sequences increases and that of the *gauche* bonds decreases. These short and disordered *trans* sequences are considered to play an important role in the remarkable increment of the intensity of the bands characteristic of the CONDIS phase immediately after the temperature reaches the crystallization point below the melting temperature. In other words, during the crystallization process, the disordered *trans* segments are speculated to grow rapidly and cooperatively from the originally existing disordered short *trans* segments in the molten state.

Structural Change in the Crystallization Process

As stated above, in a very short time, the random coils of the molten state change to the disordered *trans* sequences which transform to more regular orthorhombic-type *trans* form. This phenomenon could be detected also for HDPE and LLDPE samples. Sometimes the inhomogeneous distribution of side chain branching and molecular weight is said to disturb the clear detection of the essence of crystallization. The data obtained in this study can be used enough reasonably in the discussion of the structural change in the crystallization. The similar structural change could be observed for fully-deuterated high-density PE, the blend samples between DHDPE and LLDPE, the detailed description of which will be made in a separate paper. In the case of DHDPE/LLDPE blend sample, the IR bands characteristic of the disordered *trans* form could be observed for both the D and H components in the earliest stage of crystallization but the structural change from the disordered *trans* form to the orthorhombic-type *trans* form differs from that observed for the pure H (or D) sample, because the phenomenon of cocrystallization between the H and D chain components occurs at the same time with the disordered-to-ordered conformational transition.[23-31] In this way, the crystallization behavior observed here is not special to the samples used in this experiment but rather an essential feature common to the various types of PE samples, although the details might be different depending on the samples.

At the present stage we can not conclude definitely whether the disordered *trans* chain segments exist as a hexagonal "phase" or behave only as a supercooled state of the melt. The question whether the disordered *trans*

state corresponds to the hexagonal phase or not might be clarified by the measurement of the wide-angle X-ray scattering, for example. As already stated above, even in the molten state the *trans* and *gauche* conformational distribution may change depending on the temperature: as the temperature decreases, the *trans* isomers increase in population and the *gauche* isomers decrease. Therefore the disordered *trans* segments detected by the IR spectra might correspond to the *trans* isomers frozen in the supercooled melt. But we should also notify that the disordered *trans* bands appear even when the sample is cooled slowly from the melt (Figure 9), indicating that the disordered *trans* segments may not be necessarily the *trans* segments frozen in the supercooled melt but can be assumed as a "kinetically transient state" between the melt and the regular orthorhombic state.

It is difficult at present to choose more reasonable one between the above-mentioned two situations. Are the observed disordered *trans* segments originated from the "supercooled melt"? Do they correspond to the "metastable and transient" state produced from the increased population of the *trans* isomer in the melt? In any way, however, we may confirm definitely the following experimental fact that the random coil changes into the *trans*-rich form and transfers furthermore to the regular orthorhombic form. This can be assumed as one of the most possible and important routes of the crystallization of PE. According to the so-called Ostwald State Rule,[34,35] even in the transformation from the thermodynamically stable phase A to B, the metastable state C might appear transiently if this metastable state is kinetically more preferable than the energetically stable phase B. At the atmospheric pressure, the hexagonal phase of PE has been said to be thermodynamically metastable.[21,22] But the Ostwald's rule allows us to predict that the conformationally-disordered hexagonal phase might appear from the melt at first, if this phase grows kinetically faster, and then transforms into the more stable orthorhombic phase. The experimental data described in the previous section may be interpreted reasonably based on such an idea.

REFERENCES

1. "Crystallization of Polymers," M. Dosière, Ed., Kluwer Academic Publ., Dordrecht, 1992.
2. A special issue on crystallization of polymers, *Faraday Discuss. Chem. Soc.*, **68** (1979).
3. J. G. Fatou, "Crystallization Kinetics," in Encyclopedia of Polymer Science and Engineering, 2nd ed, Supplement Volume, John Wiley & Sons, Inc., New York, N.Y., 1989.
4. J. H. Magill, J. M. Schultz, and J. S. Lin, *Colloid Polym. Sci.*, **265**, 193 (1987).
5. M. Imai, K. Mori, T. Mizukami, K. Kaji, and T. Kanaya, *Polymer*, **33**, 4451 (1992).
6. M. Imai, K. Mori, T. Mizukami, K. Kaji, and T. Kanaya, *Polymer*, **33**, 4457 (1992).
7. B. S. Hsiao, K. H. Gardner, D. Q. Wu, and B. Chu, *Polymer*, **34**, 3986 (1993).
8. T. A. Kavassalis and P. R. Sundararajan, *Macromolecules*, **26**, 4144 (1993).
9. A. M. Jonas, T. P. Russell, and D. Y. Yoon, *Colloid Polym. Sci.*, **272**, 1344 (1994).
10. C. H. Lee, H. Saito, T. Inoue, and S. Nojima, *Macromolecules*, **29**, 7034 (1996).
11. H. Yoshida, *Thermal Analysis*, **49**, 101 (1997).
12. J. M. Schultz, *J. Polym. Sci., Polym. Phys. Ed.*, **14**, 2291 (1976).

13. J. M. Schultz, J. S. Lin, and R.W. Hendricks, *J. Appl. Crystallogr.*, **11**, 551 (1978).
14. G. Strobl and M. Schneider, *Macromolecules*, **18**, 1343 (1980).
15. T. Albrecht and G. Strobl, *Macromolecules*, **28**, 5827 (1995).
16. T. Albrecht and G. Strobl, *Macromolecules*, **29**, 783 (1996).
17. P. J.Barham and A. Keller, *J. Polym. Sci., Polym. Phys. Ed.*, **27**, 1029 (1989).
18. H. H. Song, R. S. Stein, D. Q. Wu, M. Ree, J. C. Phillips, A. LeGrand, and B. Chu, *Macromolecules*, **21**, 1180 (1988).
19. H. H. Song, D. Q. Wu, B. Chu, M. Satkowski, M. Ree, R. S. Stein, and J. C. Phillips, *Macromolecules*, **23**, 2380 (1990).
20. R. S. Stein, J. Cronauer, and H. G. Zachmann, *J. Molecular Structure*, **383**, 19 (1996).
21. S. Rastogi, M. Hikosaka, H. Kawabata, and A. Keller, *Macromolecules*, **24**, 6384 (1991).
22. M. Hikosaka, S. Rastogi, A. Keller, and H. Kawabata, *J. Macromol. Sci. Phys.*, **B31**, 87 (1992).
23. K. Tashiro, R. S. Stein, and S. L. Hsu, *Macromolecules*, **25**, 1801 (1992).
24. K. Tashiro, M. M. Satkowski, R. S. Stein, Y. Li, B. Chu, and S. L. Hsu, *Macromolecules*, **25**, 1809 (1992).
25. K. Tashiro, M. Izuchi, M. Kobayashi, and R. S. Stein, *Macromolecules*, **27**, 1221 (1994).
26. K. Tashiro, M. Izuchi, M. Kobayashi, and R. S. Stein, *Macromolecules*, **27**, 1228 (1994).
27. K. Tashiro, M. Izuchi, M. Kobayashi, and R. S. Stein, *Macromolecules*, **27**, 1234 (1994).
28. K. Tashiro, M. Izuchi, F. Kaneuchi, C. Jin, M. Kobayashi, and R. S. Stein, *Macromolecules*, **27**, 1240 (1994).
29. K. Tashiro, K. Imanishi, Y. Izumi, M. Kobayashi, K. Kobayashi, M. Satoh, and R. S. Stein, *Macromolecules*, **28**, 8477 (1995).
30. K. Tashiro, K. Imanishi, M. Izuchi, M. Kobayashi, Y. Itoh, M. Imai, Y. Yamaguchi, M. Ohashi, and R. S. Stein, *Macromolecules*, **28**, 8484 (1995).
31. K. Tashiro, *Acta Polym.*, **46**, 100 (1995).
32. K. Tashiro, S. Sasaki, and M. Kobayashi, *Macromolecules*, **29**, 7460 (1996).
33. J. D. Hoffman, *Polymer*, **23**, 656 (1982).
34. W. Ostwald, *Z. Physik. Chem.*, **22**, 286 (1897).
35. A. Keller, "Crystallization of Polymers," M. Dosière, Ed., Kluwer Academic Publ., Dordrecht, 1992, pp 1–16.